JOURNAL OF THE AMERICAN CHEMICAL SOCIETY

Article

Potent and Selective Inhibitors of 8-Oxoguanine DNA Glycosylase (OGG1)

Yu-ki Tahara, Douglas Auld, Debin Ji, Andrew A. Beharry, Anna M Kietrys, David L. Wilson, Marta Jimenez, Daniel King, Zachary Nguyen, and Eric T. Kool

J. Am. Chem. Soc., **Just Accepted Manuscript** • DOI: 10.1021/jacs.7b09316 • Publication Date (Web): 27 Jan 2018

Just Accepted

ACS Publications

Journal of the American Chemical Society is published by the American Chemical Society. 1155 Sixteenth Street N.W., Washington, DC 20036

Potent and Selective Inhibitors of 8-Oxoguanine DNA Glycosylase (OGG1)

Yu-ki Tahara,[a] Douglas Auld,[b] Debin Ji,[a] Andrew A. Beharry,[a] Anna M. Kietrys,[a] David L. Wilson,[a] Marta Jimenez,[b] Daniel King,[b] Zachary Nguyen,[b] Eric T. Kool*[a]

[a] Department of Chemistry, Stanford University, Stanford, California 94305, United States
[b] Department of Chemical Biology and Therapeutics, Novartis Institutes for Biomedical Research, 250 Mass. Ave., Cambridge, Massachusetts
*to whom correspondence should be addressed: kool@stanford.edu

Abstract

The activity of DNA repair enzyme OGG1, which excises oxidized base 8-oxoguanine (8-OG) from DNA, is closely linked to mutagenesis, genotoxicity, cancer, and inflammation. To test the roles of OGG1-mediated repair in these pathways, we have undertaken the development of noncovalent small-molecule inhibitors of the enzyme. Screening of a PubChem-annotated library using a recently developed fluorogenic 8-oxoguanine excision assay resulted in multiple validated hit structures, including selected lead hit tetrahydroquinoline **1** (IC_{50} = 1.7 μM). Optimization of the tetrahydroquinoline scaffold over five regions of the structure ultimately yielded amidobiphenyl compound **41** (SU0268; IC_{50} = 0.059 μM). SU0268 was confirmed by surface plasmon resonance studies to bind the enzyme both in the absence and presence of DNA. The compound SU0268 was shown to be selective for inhibiting OGG1 over multiple repair enzymes, including other base excision repair enzymes, and displayed no toxicity in two human cell lines at 10 μM. Finally, experiments confirm the ability of SU0268 to inhibit OGG1 in HeLa cells, resulting in an increase in accumulation of 8-oxoguanine in DNA. The results suggest the compound SU0268 as a potentially useful tool in studies of the role of OGG1 in multiple disease-related pathways.

Introduction

The consequences of DNA damage are important to many biological pathways, and are central to mutagenesis, genotoxicity, and tumorigenesis.[1-6] Among the most frequent forms of damage in DNA is 8-oxoguanine (8-OG), which is generated by reactive oxygen species arising from metabolism, or exposure to agents that induce oxidative stress.[5-17] Because 8-OG is mispaired frequently with adenine during DNA replication, it is highly mutagenic,[18] and the frequency of guanine oxidation combined with this mispairing causes it to be the greatest single source of mutations in the cell.[15] Mutations that occur in proto-oncogenes can initiate tumorigenesis,[19] and the presence of 8-OG in DNA can also be harmful to cell growth by leading to DNA double strand breaks.[20]

The primary enzyme for repairing 8-OG in DNA is 8-oxoguanine DNA glycosylase (OGG1), which functions via a base excision repair (BER) mechanism.[21] The enzyme exists both in the nucleus and mitochondria, repairing DNA damage in both subcellular locations.[22] It recognizes 8-OG in double-stranded DNA, and cleaves the glycosidic bond, releasing the 8-OG free base, and generating an abasic deoxyribose in the DNA.[21] This abasic site is then further processed by lyase activities of the enzyme itself or the AP lyase enzyme, ultimately leading to strand cleavage.[20,23,24] Additional enzymes in the BER pathway can then complete the damage repair, regenerating intact DNA with correctly paired bases.[21]

Because of the importance of OGG1 to DNA mutations and genotoxicity, a good deal of study has been devoted to investigating how varied levels of this activity can affect disease pathologies. OGG1-deficient mice display elevated levels of genomic 8-oxoguanine and increased mutations, highlighting the importance of this enzyme in maintaining genome integrity.[25,26] OGG1 mutants with abolished or decreased 8-OG repair activity have been found in many tumor specimens.[27,28] A common OGG1 polymorphism, S326C, which lowers BER activity, is positively associated with frequency of cancers of the digestive system and the lung.[29-31] In addition to its prominent association with genetic mutations leading to malignancies, OGG1-mediated repair of 8-oxoguanine has been associated with inflammation-related pathologies as well.[32] 8-OG is known to act as a signaling molecule that modulates activity of several GTPases.[33] Downregulated OGG1 activity results in decreased lung inflammation in murine allergy models.[32] Furthermore, polymorphisms in the *OGG1* gene have been associated with rheumatoid arthritis.[34]

Taken together, the data suggest strong links between OGG1 and multiple disease states. For further studies of these relationships, it would be desirable to have small molecule inhibitors of the enzyme, which could be useful as tools to study OGG1-related pathways and pathologies in cellular and animal models. The only previously known small molecule inhibitors of OGG1 were reported recently by Lloyd, who described simple hydrazine and hydrazone derivatives that inhibited the enzyme as measured by an assay that measures DNA strand cleavage subsequent to base excision.[35] Since hydrazones can spontaneously hydrolyze,[36] and hydrazines are known to react generally with abasic sites in DNA,[37,38] such classes of compounds may raise questions of stability and specificity. In general, the use of BER assays that measure DNA cleavage rather than the excision event may result in identification of hit compounds that do not act by inhibiting initial base excision.

For these reasons, discovery and development of highly potent, selective and stable small molecule inhibitors of OGG1 remain an important goal, and this goal would be aided by an assay that directly measures excision. In an effort to directly measure the base excision activity of OGG1, we recently developed fluorogenic probe (OGR1) that can detect the removal of 8-OG in real-time (Figure 1).[39] In this probe, 8-OG acts as a fluorescence quencher of a neighboring fluorescent DNA base, and enzymatic excision of the 8-OG renders the probe emissive. The fluorescent signal then yields a quantitative measurement of OGG1 activity.

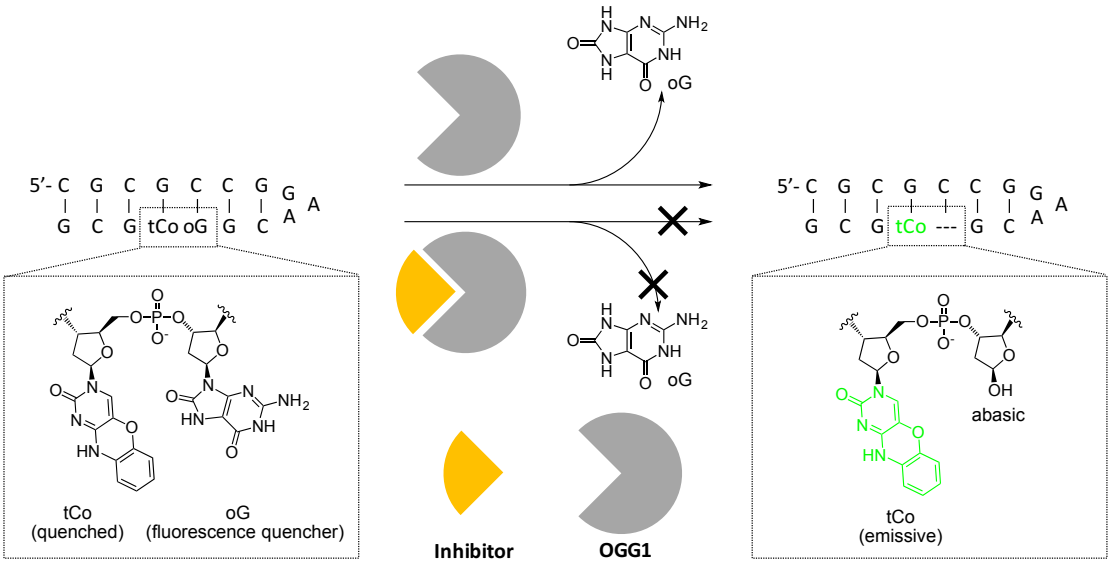

Figure 1. OGR1 probe for assay of OGG1 base excision repair activity and inhibition.[39]

Herein, we describe the development of small-molecule OGG1 inhibitors using this fluorogenic assay in high throughput, leading to the identification of a tetrahydroquinoline scaffold with significant inhibitory activity. We report structure-activity relationships of a broad set of derivatives as potential inhibitors of the enzyme, and we describe the properties of the potent and selective inhibitor SU0268 that resulted from this work.

Materials and Methods

General Information

^{1}H NMR spectra were recorded on Varian Inova 300 (300 MHz) spectrometers. The chemical shifts were reported in parts per million (δ) relative to internal standard TMS (0 ppm) for $CDCl_3$. The peak patterns are indicated as follows: s, singlet; d, doublet; t, triplet; dt, m, multiplet; q, quartet. The coupling constants, *J*, are reported in Hertz (Hz). ^{13}C NMR spectra were obtained by Varian Inova 300. $CDCl_3$ was used as a NMR solvent (Acros Organics). Low-resolution mass spectra were measured on an ESI (Electro Spray Ionization) by the ACQUITY UPLC (Waters). High-resolution mass spectra (HRMS) were measured on an ESI by micrOTOF-Q II (Bruker). Ultraviolet spectra were measured on a Varian Cary 300. Fluorescence intensities were measured on Fluoroskan Ascent Microplate Fluorometer. OGR1 probe was synthesized by using an Applied Biosystems 394 DNA/RNA synthesizer. ClogP and tPSA were calculated by ChemDraw. Analytical TLC was performed on ready-to-use plates with silica gel 60 (Merck, F254), Flash column chromatography was performed over Fisher Scientific silica gel (grade 60, 230-400 mesh). All reagents were weighed and handled in air and backfilled under argon at room temperature. Unless otherwise noted, all reactions were performed under an argon atmosphere. All chemicals were purchased from, Acros Organics, Alfa Aesar, Ark Pharm, Asta Tech, Combi-Blocks, Enamine, Matrix Scientific, Sigma-Aldrich and TCI and used without further purification.

Synthesis of compounds 2-44. Details of synthesis and characterization of these analogs and their synthetic intermediates are given in the Supporting Information file.

General procedure for OGG1 inhibitor assay. BSA, hOGG1 and NEBuffer 4 (50 mM potassium acetate, 20 mM Tris-acetate, 10 mM magnesium acetate, 1 mM dithiothreitol, pH

7.9 at 25 °C), were purchased from New England Biolabs and used. UltraPure Distilled Water (Invitrogen) was purchased and used for the assay.

Synthesized compounds and hOGG1 (100 nM) were incubated in NEBuffer 4 (1 X) with BSA (1 X) at 37 °C (15 min) in 100 µL reaction volumes in a black 96-well plate. After that, OGR1 probe[39] (1.2 µM) was added to the reaction mixture. Fluorescence at 460 nm was measured on a Thermo Fluoroskan Ascent FL fluorescence plate reader (λ_{ex} = 355 nm). The slope of initial rate (12 min) was calculated, and percent of control was used for inhibition activity.

For the HTS, the assay was optimized for 384-well plates (low volume, black solid plates, Greiner cat# 784076). For the HTS assay, 5 µL of 100nM hOGG1 was dispensed using a FlexDrop dispenser (Perkin Elmer) in NEBuffer 4. Next library plates containing compounds at 2 mM in DMSO were used to transfer 100 nL of the DMSO solution to the assay plate using an acoustic dispenser (EDC Biosystems, ATS). After a 15 min incubation at 37 °C, the enzyme reaction was started by adding 5 µL of 1.6 µM OGR1 in NEBuffer 4 using the FlexDrop. Final concentrations of OGG1 and OGR1 were then 50 nM and 0.8 µM, respectively. The reaction was incubated at 37 °C for 30 minutes and the fluorescence was determined on a Perkin Elmer Envision microtiter plate reader (λ_{ex} 340 nm and λ_{em} 450 nm using Lance/Delfia dichroic mirror of 412 nm). See Supporting information for further details.

Screening of enzyme selectivity. Details of assays for MTH1, dUTPase, NUDT16, AlkBH2, AlkBH3, and SMUG1 are given in the Supporting Information.

SPR studies. Recombinant His-tagged OGG1 (Creative Biomart) was exchanged to phosphate buffered saline (PBS). Limited biotinylation of OGG1 surface lysines was performed at 4 ^{o}C for 20 minutes using EZ-Link Sulfo-NHS-LC-Biotin (Thermo Scientific) and exchanged back to PBS on a desalting column to quench the reaction. All SPR studies were performed on a Biacore 8K instrument (GE Healthcare Life Sciences) using 50 mM potassium acetate, 20 mM Tris-acetate, 10 mM magnesium acetate, 1 mM DTT, 2% dimethylsulfoxide (DMSO) and 0.005% Tween, pH 7.9 as the running buffer. 3,000 resonance units (RU) of biotinylated OGG1 was captured on streptavidin sensor chip SA (GE Healthcare Life Sciences). Following capture, any remaining streptavidin sites on both the reference and active channels were blocked with biocytin. A 1:3 dilution series of compound **41** (highest

concentration 4 µM), prepared to match the running buffer, was flowed over OGG1. All sensorgrams shown are reference subtracted with solvent correction procedures implemented. Data were fit to both steady state and a 1:1 kinetic model using Biacore evaluation software.

Michaelis Menten kinetics studies. For Michaelis-Menten curves: Inhibitor **41** and hOGG1 (100 nM) were incubated in NEBuffer 4 (1 X) with BSA (1 X) at 37 °C (15 min) in 100 µL reaction volumes in a black 96-well plate. After that, OGR1 (0.8-10 µM) was added to the reaction mixture. Fluorescence at 460 nm was measured on a Thermo Fluoroskan Ascent FL fluorescence plate reader (λ_{ex} = 355 nm). The initial rate (10 min) was calculated.
Lineweaver-Burk plots were derived from the Michaelis-Menten curves. K_m and V_{max} were calculated from the equation. k_{cat} was calculated from $k_{cat} = V_{max}$/[enzyme].

DNA binding studies. Abasic DNA: NEBuffer 4 (1 X), 1 µM abasic DNA, 2 µM **41** (1% DMSO) were included in 1600 µL reaction volumes with 1 cm path-length quartz cells. The UV absorbance at 260 nm was measured on a Varian Cary 300 as temperature was raised 1 °C /min. The Tm value was calculated by Meltwin.
OGR1 probe: PBS buffer (0.1 X), 1 µM OGR1 probe, 2 µM **41** (10% DMSO) were included in 800 µL reaction volumes with 1 cm path-length quartz cells. The UV absorbance at 260 nm was measured on a Varian Cary 300 as temperature was raised 1 °C/min. The Tm value was calculated by Meltwin.

Toxicity via MTT assay. HEK293T cells (1.6×10^4 cells per well) and HeLa cells (concentration of 1.2 × 10^4 cells per well) were seeded to 96-well plate in supplemented DMEM culture medium (10% FBS, 100U Penicillin/Streptomycin) and incubated for 30 h (HEK293T cells) and 16 h (HeLa cells) at +37 °C, 95% humidity and 5% CO_2. They were incubated in 100 µl of the fresh medium at a concentration of 100 µM, 10 µM, 1 µM, 100 nM, and 10 nM of the compound **41** for 24 h at +37°C, 95% humidity and 5% CO_2, in supplemented DMEM culture medium. After the incubation period, 10 µL of the MTT labeling reagent (final concentration 0.5 mg/mL) was added to each well, and incubated at +37°C, 95% humidity and 5% CO_2. 100 µL of the solubilization solution was added into each well, and incubated for 20 h at +37 °C, 95% humidity and 5% CO_2. Absorbance of the samples was measured by using a microplate

reader (Tecan Infinite M1000) at 550, and 650 nm. Compound **41** was provided in concentration of 2 mM in DMSO that determined final concentration of DMSO in 100 µM at the level of 5%. In the remaining samples (10 µM, 1 µM, 100 nM, 10 nM) concentration of DMSO was at the level of 1%. The controls were prepared: Ctrl – cells cultured only in the supplemented DMEM; Ctrl 5% DMSO - cells cultured in 5% DMSO in the supplemented DMEM; Ctrl 1% DMSO - cells cultured in 1% DMSO in the supplemented DMEM.

Detection of 8-OG in cell line by LC-MS/MS. HeLa cells (2×10^6 cells per well) were seeded in 10 cm dishes in supplemented DMEM culture medium (10% FBS, 100U Penicillin/Streptomycin) and incubated for 12 h (HeLa cells) at +37 °C, 95% humidity and 5% CO_2. They were incubated in 10 mL of the fresh medium at a concentration of 5 µM and 0.5 µM of compound **41** for 24 h at +37°C, 95% humidity and 5% CO_2, in supplemented DMEM. Every 6 h fresh medium with the compound **41** was added. Control HeLa cells were cultured in supplemented DMEM culture medium. For positive oxidative damage controls, we cultured HeLa cells in the supplemented DMEM medium with 0.5 mM H_2O_2 and 0.3 mM $CrCl_3$. After incubation, all cells were washed twice with PBS and harvested for DNA isolation. DNA isolation was performed with Quick-DNA™ Miniprep Plus Kit (Zymo Research) according to the manufacturer's protocol. The concentration of DNA eluted in nuclease-free water was measured on a NanoDrop One instrument (Thermo Scientific). The DNA (5 µg) was dried and then digested with 0.02 U spleen II nuclease (Worthington) and 0.4 U micrococcal nuclease (Sigma Aldrich) in 20 mM succinate buffer containing 10 mM $CaCl_2$ for 16 h at 37 °C. The hydrolysate was treated with 0.4 µg RNase P1 (Sigma Aldrich) in 78 mM ammonium acetate buffer (pH 4.5) and 10 mM bicine-NaOH buffer (pH 9.7) containing 10 mM $MgCl_2$, 10 mM dithiothreitol, and 1 mM spermidine for 6 h at 37 °C. The final volume of the mixture was 25 µL. 75.5 µL internal standard was added to all samples and blank sample to a total volume of 100 µL. One of the blank samples was prepared without internal standard. The reaction mixtures were filtered through Amicon Ultra 0.5 mL 3 kDa cut-off filters (Millipore). The set of 12 spiking solutions, containing dG, dC, 8oxodG, was prepared according to the digestion procedure for DNA. The detection range covered by spiking solution was: 0.0625 ng/mL to 100 ng/mL for 8-oxodG, and 2.5 ng/mL to 5.97 µg/mL for dG. Additionally, in the LC-MS/MS analysis internal standards of [$^{15}N_5$] dG and [$^{15}N_3$] dC were used. The nucleosides were separated on a Synergi 4 µm Fusion column, RP 80 Å, 150 x 2

mm, at 30 °C with 10 µL injection volume, and flow rate of 200 µL/min. Separation was performed using following program: 0-3 min 100% phase A (0.1% formic acid in water), 9 min 60% phase A and 40% phase B (0.1% formic acid in acetonitrile), 12 min 10% phase A, 12.1 – 15 min 100% phase A. Collected values of 8-oxodG content (ng/mL) were normalized to the amount of dG for all replicates.

Inhibition of OGG1 activity in cell lysates by SU0268. HeLa and MCF-7 cells were seeded in 15 cm dishes in supplemented DMEM culture medium (10% FBS, 100U Penicillin/Streptomycin) (Gibco) and incubated for 48 h at +37 °C, 95% humidity and 5% CO_2 to full confluence. Cells were scraped, washed with 1 x PBS (pH 7.4) and decanted. For each cell culture the packed cell volume (PCV) was estimated. The 5 x PCV of lysis buffer (10 mM HEPES pH 7.9 (Gibco), with 1.5 mM $MgCl_2$ (Sigma Aldrich) and 10 mM KCl (Sigma Aldrich), 1 mM DTT (Invitrogen), 1 x Protease Inhibitor Cocktail (Roche)) was used to resuspend cells. The suspension was incubated on ice for 15 min to allow cells to swell, and then centrifuged for 5 minutes at 420 x g, at 4°C. The cell pellet was resuspended in 2 x PCV of lysis buffer and lysed using a syringe with a narrow-gauge (No. 25) hypodermic needle. Disrupted cells were centrifuged 20 minutes at 11,000 x g, at 4°C. The collected supernatant was the cytoplasmic fraction. The nuclei pellet was resuspended in 2/3 x PCV of extraction buffer (20 mM HEPES pH 7.9 (Gibco), with 1.5 mM $MgCl_2$ (Sigma Aldrich), 0.42 M NaCl (Sigma Aldrich), 0.2 mM EDTA (Invitrogen), 25% (v/v) Glycerol (Sigma Aldrich), 1 mM DTT (Invitrogen), 1 x Protease Inhibitor Cocktail (Roche)), and shaken for 60 min at. at 4°C. The suspension was centrifuged for 5 min at 21,000 x g, at 4°C, and the supernatant containing nucloplasmic fraction was collected. Two volumes of cytoplasmic fraction were mixed with one volume of nucleoplasmic fraction and this protein mixture was used in the experiment. Concentration of proteins was measured using the Bradford Protein Assay (Biorad) according to the manufacturer's protocol. Reactions were performed with a total volume of 80 µL containing 100 ng/µL total cell protein, 2 µM pOGR1 probe, and 10 mM $MgCl_2$, and were incubated for 24 h at 37°C in a black 384-well plate. Fluorescence was measured at 460 nm using a Fluoroscan Ascent FL plate reader (Thermo Scientific) and excitation wavelength 355 nm.

Procedure for CACO-2 assay. Measurements were carried out by Absorption Systems LLC. See Supporting Information for experimental details.

Results and Discussion

Small molecule screening for OGG1 inhibition. The identification of OGG1 inhibitors was initiated with a high-throughput screen of the PubChem-annotated library compounds using hOGG1 enzyme and our originally developed OGR1 probe assay, using recombinant human OGG1. Approximately 26,000 compounds were chosen for initial screening, and the assay was carried out at a single 20 μM concentration (Figure 2). The high-throughput screen showed good performance with a Z′ = 0.68±0.1 and led to over 350 initial hit compounds using a threshold of >35% inhibition, which was >3 s.d. of the maximum enzyme activity controls treated with DMSO vehicle alone. The hit compounds showed varied chemical structures and were then further validated by titration over an 8-fold concentration range to determine IC_{50} values. The assay yielded several validated hit compounds, from which we selected compound **1**, a tetrahydroquinoline sulfonamide derivative, for further study. Compound **1** did not score as active in another fluorescence enzyme assay which used the same fluorescence detection protocol,[40] thus confirming that its activity was not a false positive resulting from inherent fluorescence. In addition, compound **1** (annotated in PubChem as CID:7517554) has been tested in 84 assays. Of these assays, only two listed the compound as active, with no IC_{50}'s below 10 μM, supporting a selective compound profile.

Our general strategy for structural optimization of scaffold **1** is shown in Figure 2. The chemical structure of **1** was divided into five fragments A-E; fragment B consists of the core tetrahydroquinoline structure, and A is a substituent on the nitrogen atom of this core structure. Fragment C, a sulfonamide, is a linker between core structure B and fragment D, a benzene ring. Fragment E is a substituent of this aromatic ring. We varied these five fragments to investigate their influences on OGG1 base excision as measured by the OGR1 assay.

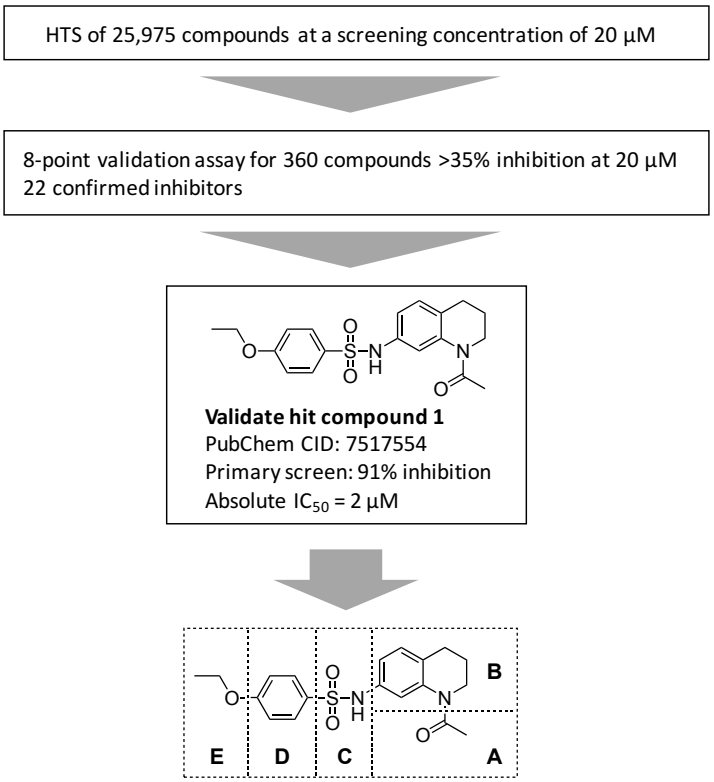

Figure 2. Discovery of lead compound **1** and strategy for the lead optimization. Following the HTS compounds were validated using eight concentration points ranging from 100 to 0.03 µM. Absolute IC_{50} is the concentration for which the concentration response curve crosses 50% inhibition.

Structural optimization. For the initial optimization studies, we synthesized analogs of hit compound **1** with varied substituents (R^1) on the nitrogen atom of the tetrahydroquinoline skeleton (Table 1). Assays of these compounds were carried out over a three-log concentration range to differentiate weak inhibitors from stronger ones. Lead compound **1** (with acetamide substituent as R^1) showed significant inhibition of OGG1 at 20 µM and ca. 50 % inhibition at 2 µM, but yielded little inhibition activity at 200 nM. Homologation of acetamide to ethylamide (**2**) had little effect on inhibition, while larger substituents (**3**-**6**) lowered the activity. Interestingly, however, cyclopropylamide analog **7** showed significantly more potent inhibition activity than the lead compound (Table 6), and was also more active than the closely related isopropyl variant **5**. A slightly larger ring (cyclobutyl compound **8**) showed somewhat lower potency. We proceeded to other R^1 substituents, varying the carbonyl itself. Sulfonamide analog **9**, urea analog **10** and reduced analog **11** were prepared and assayed. However, these compounds showed little or no activity at 20 µM. These results establish that the carbonyl group on the tetrahydroquinoline nitrogen atom is highly

important for activity, and among them, the cyclopropylamide group was the optimal substituent for R^1.

Table 1. Examination of substituents R^1 and their effects on OGG1 activity (Fragment A)

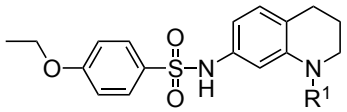

Cmpd	R^1	Enzyme activity, % of control at 20 μM[a]	2 μM[a,b]	200 nM[a, b]
1		4.7 ± 3.0	47 ± 3.5	74
2		3.7 ± 0.83	51 ± 1.4	n.t.
3	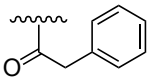	79	≥ 100	n.t.
4	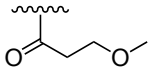	51	93	n.t.
5		52	96	n.t.
6		≥ 100	n.t.	n.t.
7	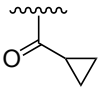	5.8 ± 1.9	41 ± 1.7	82 ± 12
8	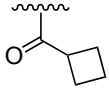	33	69	n.t.
9	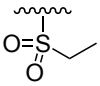	92	96	n.t.
10	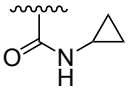	77	87	n.t.
11		83	≥ 100	n.t.

[a] % of control values are ratio of enzyme activity to control (no compound) based on slopes of initial rate (first 12 min of assay). [b] n.t., not tested.

Next, we examined fragment B, the core structure of the initial hit compound (Table 2). Acyclic compound **12** and 5-membered ring dihydroindole **13** showed low activity. The 7-

membered ring analog **14** was also examined, but displayed lower inhibition activity than the 6-membered ring analog **7** shown in Table 1. To test the effects of the carbon skeleton of the tetrahydropyridine ring, we introduced an oxygen atom (**15**), but this showed lower inhibition, suggesting a relatively hydrophobic contact with the enzyme at this position. We installed a methoxy substituent on the benzene ring of the tetrahydroquinoline skeleton (**16**), but this almost completely abrogated inhibitory activity. Finally, we repositioned the cyclopropylamide substituent by one atom in the tetrahydroisoquinoline derivative **17**, but this also greatly lowered activity. These data establish that the tetrahydroquinoline skeleton is quite important to the inhibitory activity of active compounds **1** and **7**.

Table 2. Examination of core structure R^2 and their effects on OGG1 activity (Fragment B)

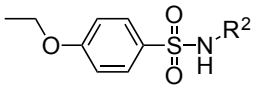

Cmpd	R^2	Enzyme activity, % of control at 20 μM[a]	2 μM[a,b]	200 nM[a, b]
1	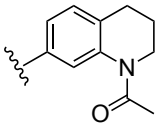	4.7 ± 3.0	47 ± 3.5	74
7	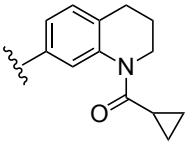	5.8 ± 1.9	41 ± 1.7	82 ± 12
12	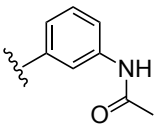	70	96	n.t.
13	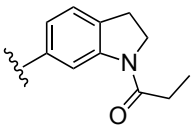	≥ 100	95	n.t.
14	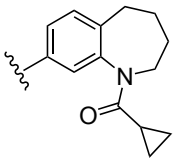	35	76	n.t.
15	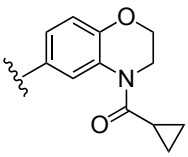	41	90	n.t.

16	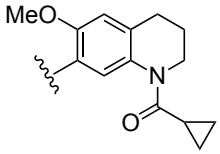	93	≥ 100	n.t.
17	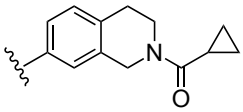	88	94	n.t.

[a] % of control values are ratio of enzyme activity to control (no compound) based on slopes of initial rate (first 12 min of assay). [b] n.t., not tested.

We proceeded to test variations of Fragment C, the sulfonamide linker between the tetrahydroquinoline and the aromatic substituent, preparing diverse linkers in compounds **18**-**21** (Table 3). *N*-hydroxy and *N*-methyl groups combined with sulfonamide (**18** and **19**) were tested, but they showed lower inhibition activity than unsubstituted sulfonamide **7** (Table 1). This suggests possible polar interactions in the enzyme with the N-H group. Amide and urea analogs (**20** and **21**) were synthesized and assayed, but showed almost no activity. Therefore, the simple "N-H" benzenesulfonamide structure in Fragment C was selected as most appropriate for further studies.

Table 3. Examination of linker R^3 and their OGG1 inhibition activity (Fragment C)

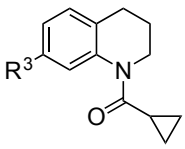

Cmpd	R^3	Enzyme activity, % of control at 20 μM[a]	2 μM[a,b]	200 nM[a, b]
1		4.7 ± 3.0	47 ± 3.5	74
7	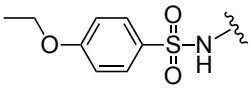	5.8 ± 1.9	41 ± 1.7	82 ± 12
18	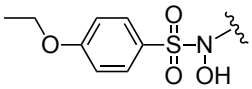	21	79	≥ 100
19	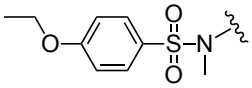	79	84	n.t.
20	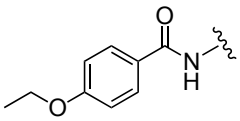	≥ 100	≥ 100	n.t.

21	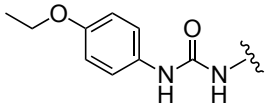	≥ 100	≥ 100	n.t.

[a] % of control values are ratio of enzyme activity to control (no compound) based on slopes of initial rate (first 12 min of assay). [b] n.t., not tested.

We next investigated the effects of variations of Fragments D and E of the core structure (Table 4). Ethyl sulfonamide derivative **22** proved to be quite poorly active, suggesting the importance of the aromatic framework. Subsequently, a variety of substituents on the benzene ring were prepared and assayed with OGG1 and the OGR1 probe. Compound **23**, carrying a 4-propylphenyl substituent, showed inhibition activity nearly the same as that of compound **7** possessing 4-ethoxyphenyl group. Compound **24**, which extends the alkyl chain compared with **7** was tested, but this did not improve activity. The analogs possessing nitrogen and sulfur atoms on the benzene ring were tested, but the heteroatoms had slightly deleterious effects on activity (**25** and **26**). The disubstituted compound **27** showed lower inhibition activity than mono-substituted compound **7**. Unexpectedly, testing of compound **28** which has a diphenyl ether group, showed almost the same activity as compound **7** with its ethoxy group. Therefore, we designed and synthesized the dibenzofuranyl analog **29** and biphenyl analog **30**, which are rigidified variants of the diphenyl ether compound. Interestingly, compound **29** showed low activity, but compound **30** had more potent activity than either diphenyl ether **28** and ethoxyphenyl compound **7**. Cyclohexylphenyl derivative **31** showed almost the same activity as biphenyl derivative **30**, but a more polar morpholinophenyl substituent (**32**) had a poor effect on the activity. Pyrazolylphenyl and pyridylphenyl analogs (**33** and **34**) containing a polar nitrogen atom were subjected to the assay. We found that compound **34** gave slightly stronger inhibitory activity than biphenyl compound **30**, displaying ca. 60% inhibition of activity at 200 nM.

Table 4. Examination of substituents R^4 and their effects on OGG1 activity (Fragments D, E)

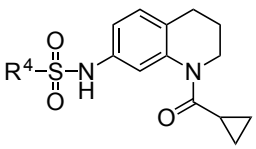

Cmpd	R^4	Enzyme activity, % of control at 20 μM[a]	2 μM[a,b]	200 nM[a, b]
1		4.7 ± 3.0	47 ± 3.5	74
7	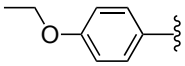	5.8 ± 1.9	41 ± 1.7	82 ± 12
22[c]		74	94	n.t.
23	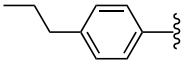	14	35	74
24	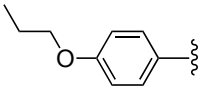	n.t.	19	95
25	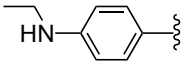	10	58	≥ 100
26	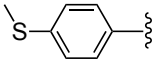	3.6	53	75
27	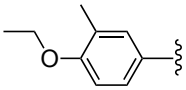	22	71	n.t.
28	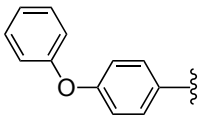	8.3	41 ± 2.0	≥ 100
29	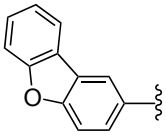	71	82	n.t.
30	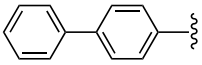	n.t.	29 ± 7.0	90 ± 6.2
31	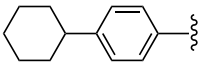	n.t.	25	87
32	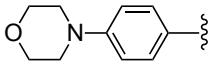	n.t.	76	84
33	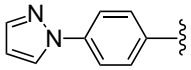	14 ± 3.2	45 ± 1.3	81
34	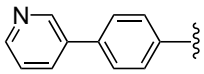	2.0	23 ± 1.5	61 ± 1.3

[a] % of control values are ratio of enzyme activity to control (no compound) based on slopes of initial rate (first 12 min of assay). [b] n.t., not tested. [c] Acyl group of nitrogen atom on tetrahydroquinoline skeleton is propionyl group.

Finally, we explored structural effects of the substituents on the terminal aromatic ring of lead compound **30**, synthesizing compounds **35**-**39** (Table 5). When 4-trifluoromethyl as an electron withdrawing group and 4-methoxy as an electron donating group were compared (**35** and **36**), the more polar and electron-donating group (4-methoxy) assisted the activity more than the electron-withdrawing group. Moving this substituent's position,

the 3-methoxy compound **37** resulted in more potent activity than the 4-substituted compound **36**. Therefore, varied substituents at the *meta*-position of this benzene ring were examined. Compound **38** (with a dimethylamino group) and compound **39** (possessing an acetylamino group) were synthesized and assayed. The compound **38** showed similar activity as methoxy compound **37**, but the acetamide **39** showed higher activity than either of these, with inhibition activity of about 50 % at 200 nM. When we investigated the compounds **40** and **41** which have reverse amide structure, these compounds showed yet higher activity, and compound **41** (SU0268), possessing a *meta*-carboxamide group, had the strongest inhibitory activity of all compounds in the study.

Table 5. Examination of substituents R^5 and their OGG1 inhibition activity (Fragment E)

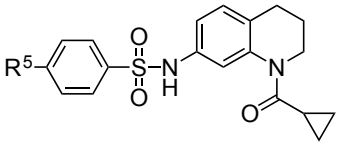

Cmpd	R^5	Enzyme activity, % of control at 20 μM[a,b]	2 μM[a,b]	200 nM[a]
1		4.7 ± 3.0	47 ± 3.5	74
7		5.8 ± 1.9	41 ± 1.7	82 ± 12
35	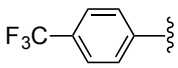	n.t.	72	97
36	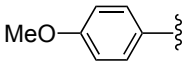	n.t.	31	79
37	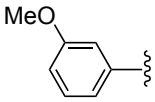	n.t.	13	67
38	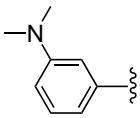	n.t.	n.t.	70
39	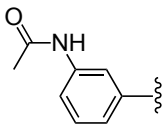	n.t.	12 ± 2.0	53 ± 4.9
40	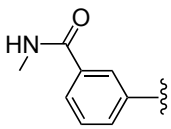	n.t.	n.t.	48
41	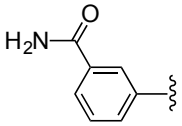	n.t.	4.8	39 ± 2.5

[a] % of control values are ratio of enzyme activity to control (no compound) based on slopes of initial rate (first 12 min of assay). [b] n.t., not tested.

Synthesis of SU0268 (inhibitor 41). The synthesis of tetrahydroquinoline biphenyl sulfonamide derivative **41**, the most potent OGG1 inhibitor in this study, is depicted in Scheme 1. We commenced the preparation of **41** with acylation of the commercially available tetrahydroquinoline **42** with cyclopropylcarbonyl chloride in the presence of *N*,*N*-diisopropylethylamine.[41] Subsequent 1-atm hydrogenation of the acylated intermediate in the presence of palladium on carbon gave the amine **43** in 77%.[41] Sulfonylation of **43** with 4-bromobenzene sulfonylchloride afforded the sulfonamide **44** in excellent yield.[42] Construction of the biphenyl structure using Suzuki-Miyaura coupling in the last step with 3-aminocarbonylphenyl boronic acid in the presence of tetrakis(triphenylphosphine)palladium(0) gave the desired **41** in 82%.[43] The intermediates **43** and **44** were obtained by crystallization, and this protocol required only one silica column chromatography purification step to isolate **41**.

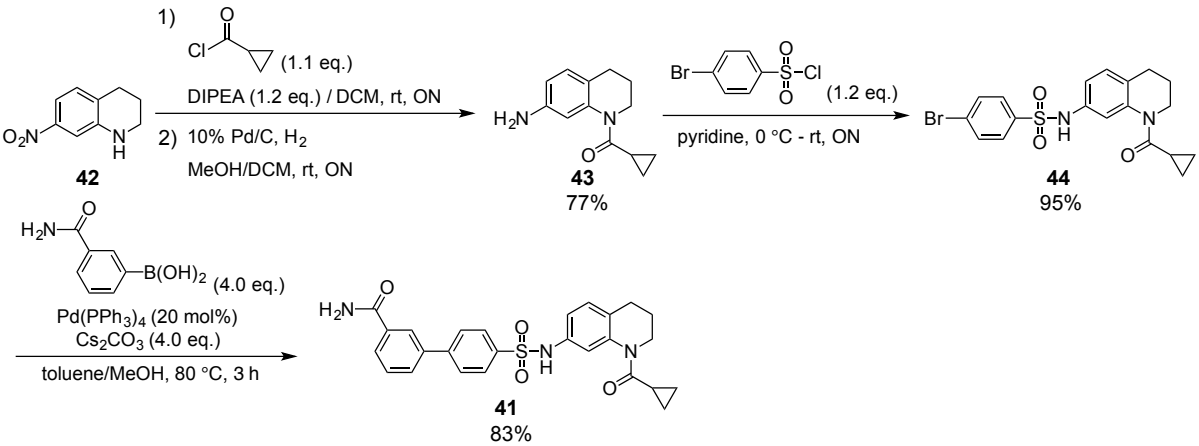

Scheme 1. Synthesis of the OGG1 inhibitor SU0268 (**41**).

Properties of selected inhibitors. Properties of selected inhibitors were further examined. Titration curves and IC_{50} values of the hit compound **1**, selected key intermediate inhibitors (**7**, **28**, **34** and **39**) and optimized compound **41** were determined using the initial rates method (Figure 3 and Table 6). The IC_{50} of the hit compound **1** was 1.7 μM. The IC_{50} values of compounds **7** and **28**, with modified substituents on tetrahydroquinoline and benzensulfonamide, were slightly more potent than that of **1**. The compounds **34** (with

pyridine ring) and **39** (with acetylamino group) had considerably higher activity than the lead compound **1**, with IC_{50} values below 0.3 μM. The IC_{50} value of the optimized compound **41** was 0.059 μM. We calculated cLogP (hydrophobicity) and tPSA (topological polar surface area) values for the compounds (Table 6) as useful measures of potentially bioactive compounds.[44,45] The values of clogP of the compound **7** and **28** were higher than the hit compound **1**, but their values of tPSA were almost the same. Our potent inhibitors **34**, **39** and **41** showed moderate cLogP values (3.4-3.8), and their tPSA values were 79-110, which also fall in the generally accepted range for potential bioactivity.[44,45]

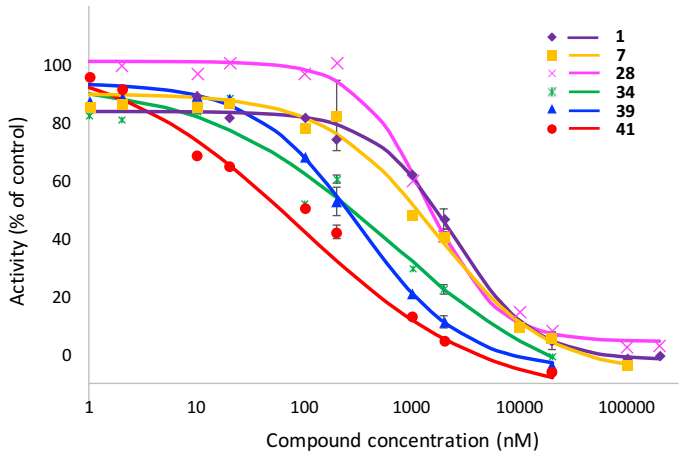

Figure 3. Titration curves of selected OGG1 inhibitors in this study

Table 6. IC_{50} of OGG1 inhibitors, and their cLogP and tPSA

Cmpd	IC_{50} (μM)	cLogP[a]	tPSA[a]
1	1.7	2.5	76
7	1.1	3.6	76
28	1.5	4.9	76
34	0.27	3.4	79
39	0.25	3.8	96
41	0.059	3.3	110

[a] see SI for calculation methods.

Surface plasmon resonance (SPR) was used to validate the series and confirm the compounds acted through OGG1. Compound **41** was titrated against biotinylated OGG1 previously captured on a SA streptavidin sensor chip (Figure 4). Sensorgram plots showed a

saturable dose response consistent with specific binding to OGG1. The data, fit against 1: 1 kinetic and steady state models, gave K_d's consistent with IC_{50} of the biochemical assay.

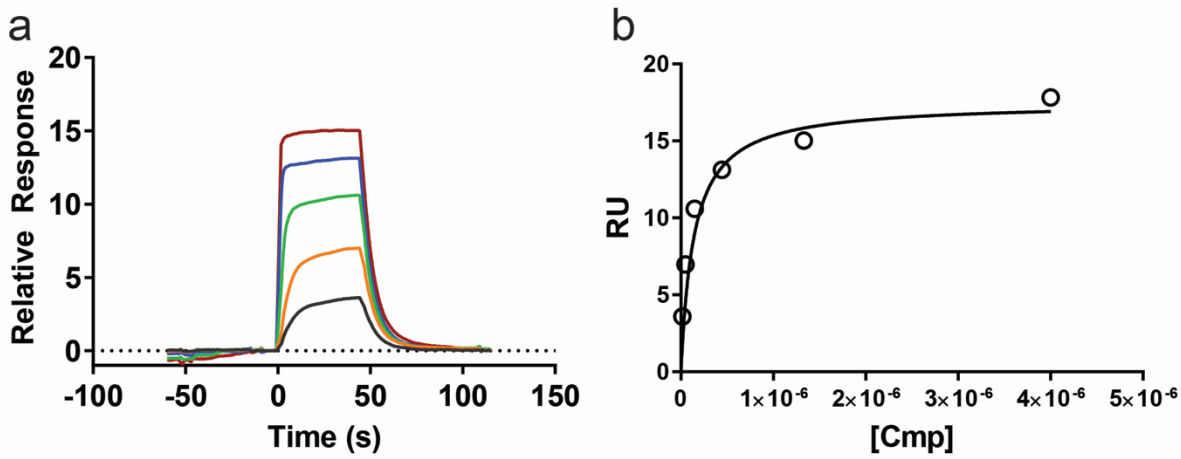

c

k_a (M^{-1} s^{-1})	k_d (s^{-1})	$K_D = k_d/k_a$ (M)	Steady State K_D (M)
1.4×10^6	0.23	1.6×10^{-7}	2.1×10^{-7}

Figure 4. SU0268 (**41**) specifically binds OGG1. 3000 RU (Resonance Units) of recombinant biotinylated OGG1 was immobilized onto streptavidin sensor chip SA and experiments were performed on a Biacore 8K with a 1:3 dilution series of inhibitor **41** (highest concentration 4 μM) (**a**) Sensorgram plots of inhibitor **41**. (**b**) Steady state K_d determination of compound **41**. (**C**) Kinetic and binding constants.

To investigate the effects of SU0268 on inhibition of OGG1, we measured Michaelis-Menten parameters in the absence and presence of this compound at 200 nM and 2 μM. A Lineweaver-Burk plot was obtained from Michaelis-Menten curves (Figure 5), and K_m and k_{cat} values were calculated (Table 7). Measuring the effect of the inhibitor showed an increase in K_m and little or no effect on k_{cat}. These results indicate that inhibitor **41** acts as a competitive inhibitor against OGG1.[46]

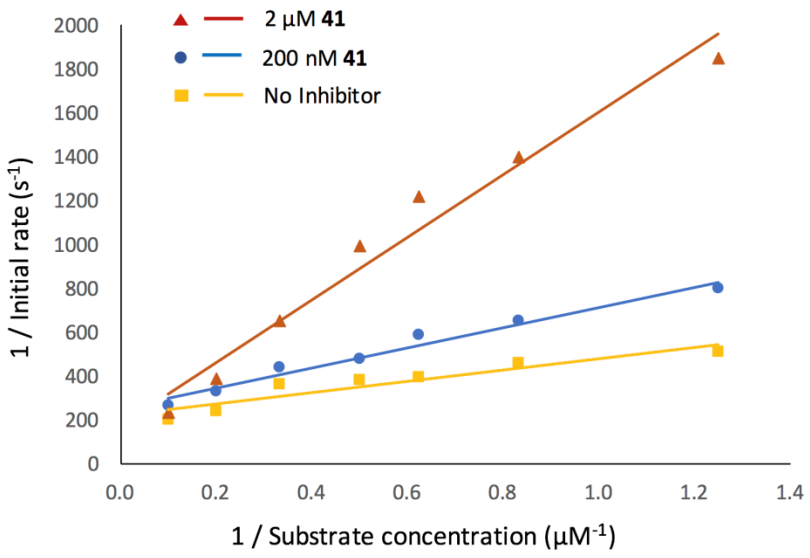

Figure 5. Lineweaver-Burk plots of OGG1 activity without inhibitor and with inhibitor **41**

Table 7. K_m and k_{cat} without inhibitor and with inhibitor **41**

	No Inhibitor	200 nM **41**	2 μM **41**
K_m (μM)	1.2	1.8	8.2
k_{cat} (s^{-1})	0.046	0.040	0.057
k_{cat}/K_m ($s^{-1}\mu M^{-1}$)	0.039	0.022	0.0070

We further investigated interaction of abasic DNA (without 8-OG) and OGR1 probe (with 8-OG) with inhibitor **41** (Table 8). Abasic DNA has C instead of tCo and was introduced abasic site mimic (X) instead of 8-OG. If the interaction is observed, melting temperature (T_m) would be changed significantly.[47] In both cases of abasic DNA and OGR1 probe, no measurable changes of T_m were observed, providing evidence that inhibitor SU0268 does not bind DNA, and thus interacts with OGG1 specifically rather than its substrate.

Table 8. Thermal denaturation studies of OGR1 probe and Abasic DNA in the absence ($T_{m(-)}$) and presence ($T_{m(+)}$) of OGG1 inhibitor **41**

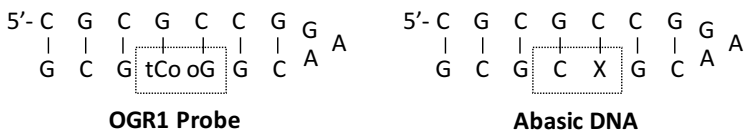

OGR1 Probe **Abasic DNA**

DNA	$T_{m(-)}$ / ˚C	$T_{m(+)}$ / ˚C	ΔT_m / ˚C
Abasic DNA[a]	71.3 ± 0.63	71.3 ± 0.29	0.0
OGR1 Probe[b]	82.2 ± 0.77	82.5 ± 0.25	0.3

[a] [DNA] = 1 μM, [**41**] = 2 μM (1% DMSO), NEBuffer. [b] [DNA] = 1 μM, [**41**] = 2 μM (10% DMSO), PBS buffer and betaine (10 mM).[48]

The selectivity of inhibitor SU0268 (**41**) was investigated by testing it against other repair enzymes that process either 8-oxoguanine nucleotides, bind nucleotides or DNA, or employ base excision mechanisms. MTH1 (human MutT Homolog 1),[49] dUTPase (Deoxyuridine 5'-Triphosphate Nucleotidohydrolase),[50] NUDT16 (Nucleoside Diphosphate linked moiety X-type motif 16),[51] hABH2 (Human AlkB Homolog 2),[52] hABH3 (Human AlkB Homolog 3),[53] and SMUG1 (Single-strand Selective Monofunctional Uracil DNA Glycosylase)[54] were assayed with the compound at 20 μM (Figure 6). The activities against all enzymes of compound **41** were low or negligible, thus establishing high selectivity of compound **41** to OGG1.

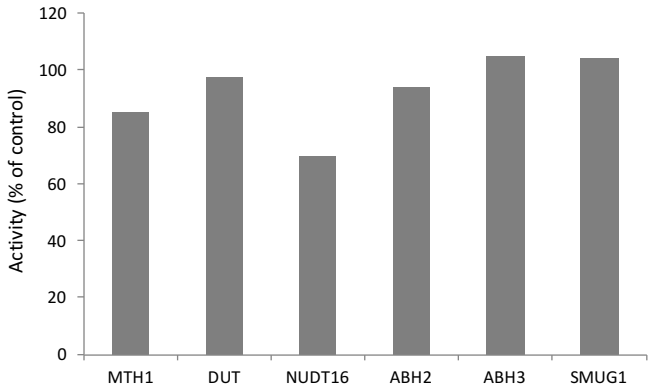

Figure 6. Selectivity of compound **41**, tested by assaying against varied repair enzymes at 20 μM.

The toxicity of compound **41** was tested in two human cell lines (HEK293T and HeLa) by the MTT assay (Figure 7). The compound showed little or no cytotoxicity in both cell lines at concentrations 10 nM to 10 µM, and exhibited moderate apparent toxicity only at the highest 100 µM concentration (30-50% toxicity). Thus, the compound is not significantly toxic at concentrations well above its IC_{50}.

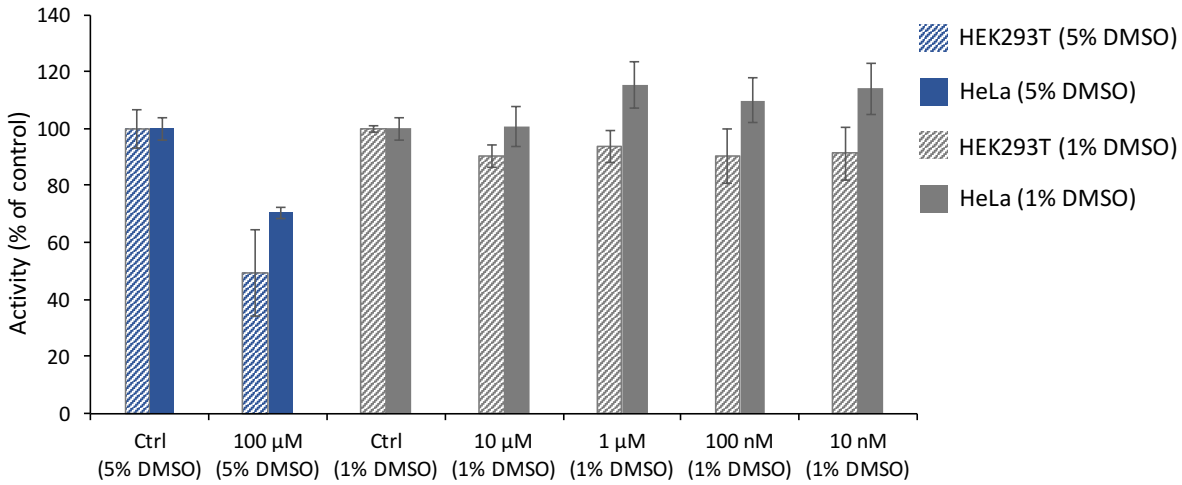

Figure 7. Toxicity of **41** (SU0268) by MTT assay with HEK293T and HeLa cell lines

Next, we examined the membrane permeability of SU0268 (**41**) using the Caco-2 (clone C2BBel) assay, measuring permeability in both the apical-to-basolateral and basolateral-to-apical directions (Table 9). Recoveries based on the apical side (A-to-B) and basolateral side (B-to-A) were 65% and 79%, showing that the permeability of compound **41** is satisfactory.

Table 9. CACO-2 assay with the OGG1 inhibitor **41**

Direction	Recovery (%)	P_{app} (10^{-6} cm/s)			Efflux Ratio
		R1	R2	AVG	
A-to-B	65	14.2	10.8	12.5	6.2
B-to-A	79	63.5	91.3	77.4	

Finally, we carried out tests of the ability of SU0268 to engage OGG1 and inhibit its activity in a human cell line. Since the cellular role of the enzyme is to remove 8-oxoG from DNA, inhibition of the enzyme is expected to measurably increase levels of the damaged

base in DNA. To evaluate this possibility, we incubated cells for 24 h with or without SU0268 at 0.5 μM, and used LC/MS-MS methods to measure levels of this damaged base in DNA isolated from the cells. The results (see Figure 8a) confirm that the drug increases levels of 8-oxodG in DNA by 25% after only 24 h relative to the mock-treated controls. The amount of increase is similar to or greater than that provided by a positive control of oxidatively damaging conditions. We also employed a fluorescence probe of OGG-1 activity[39] to directly test the ability of SU0268 to inhibit OGG1 activity in HeLa and MCF-7 tumor cell lines, which have relatively low and high OGG1 activities, respectively. Results of the assay are shown in Fig. 8b; the data confirm the inhibition of OGG1 activity at 0.5 μM of the compound, amounting to 64% and 95% inhibition of signal in the two lysates as measured at 20 h. Thus, the collective data provide evidence that SU0268 (**41**) can be active at the intended cellular target, both in lysates and in living cells.

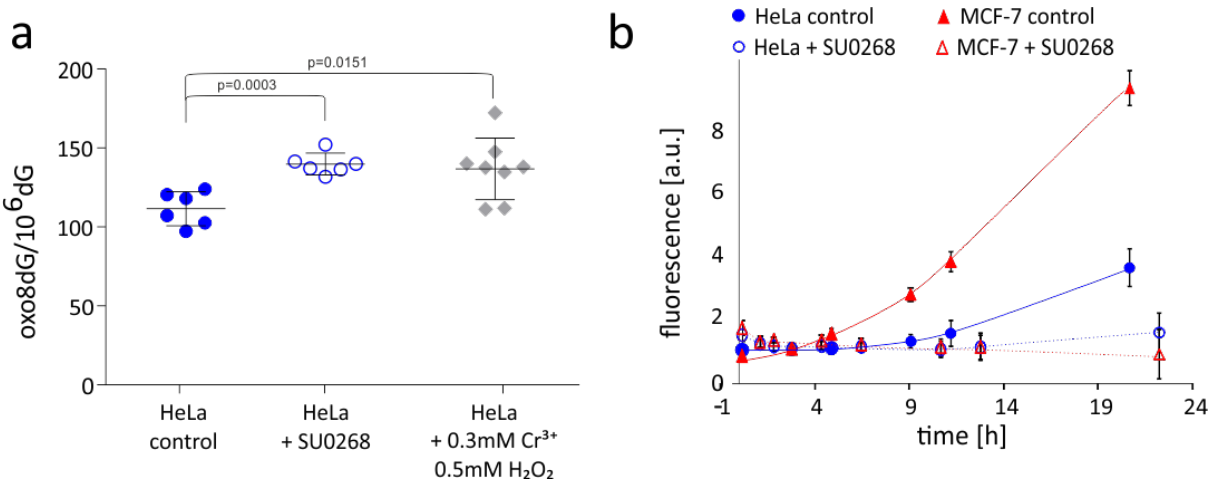

Figure 8. Inhibition of cellular OGG1 activity by **41** (SU0268). **(a)** Incubation with 0.5 μM SU0268 increases the number of oxo8dG lesions in HeLa cell DNA. **(b)** SU0268 (0.5 μM) inhibits OGG1 activity as measured by fluorescence probe (pOGR1)[39] in HeLa and MCF-7 cell lysates.

A previous report described the discovery of hydrazine and hydrazone inhibitors of OGG1 using a DNA strand cleavage assay.[35] We independently confirmed that two of the most potent of those compounds are indeed inhibitors of the enzyme *in vitro* (SI Figure S1) using our base excision (OGR1) assay. The results show that the new compound SU0268 (**41**) (IC_{50} = 0.059 μM) is more potent than those prior compounds as measured by the initial rates method. Notably, the prior compounds exhibit apparently delayed kinetics of inhibition, which suggests the possibility that the enzyme may first excise the 8-OG base before the compounds can be active (see SI Figure S1). In contrast, as measured by the

OGR1 assay, the current inhibitor SU0268 binds directly to OGG1 enzyme even in the absence of DNA, and directly inhibits base excision, the first step of repair of this lesion by this enzyme.

In summary, we have developed highly potent and selective OGG1 inhibitor SU0268 which has an acyl tetrahydroquinoline sulfonamide skeleton. The structure-activity relationships of the compounds were outlined by synthesizing a broad range of analogs. Synthesis of the optimized OGG1 inhibitor is quite straightforward from commercially available stating materials. The compound shows good membrane permeability and no cytotoxicity in HEK293T and HeLa cells at active concentrations, and demonstrates activity in inhibiting the enzyme in human cell lines. Further studies are being directed to applications of this inhibitor in varied cellular and animal models of multiple diseases.

Acknowledgement. We thank the U.S. National Institutes of Health (CA217809, GM067201, GM110050) for support, and the Ajinomoto Corporation for providing postdoctoral support to Y.T. A.A.B was supported by a postdoctoral fellowship from the Human Frontiers Science Program. We thank the Vincent Coates Foundation Mass Spectrometry Laboratory, Stanford University Mass Spectrometry for assistance with mass spectrometry measurements. We thank Kirk Wright (NIBR) for providing SPR resources. We also acknowledge Ann Schlesinger at NIBR and Stanford ChEM-H for supporting the research collaboration.

References

(1) Helleday, T.; Petermann, E.; Lundin, C.; Hodgson, Ben; Sharma, R. A. *Nat. Rev. Cancer* **2008**, *8*, 193-204.

(2) Phillips, D. H.; Arlt, V. M. *Molecular, Clinical and Environmental Toxicology*, Springer, Basel, **2009**, 87-110.

(3) Dietlei, F.; Thelen, L.; Reinhardt, H. C. *Cell Press* **2014**, 326-339.

(4) Kelley, M. R.; Logsdon, D.; Fishel, M. L. *Future Oncol*. **2014**, *10*, 1215-1237.

(5) Gavande, N. S.; VanderVere-Carozza, P. S.; Hinshaw, H. D.; Jalal, S. I.; Sears, C. R.; Pawelczak, K. S.; Turchi, J. J. *Pharmacology & Therapeutics* **2016**, *160*, 65-83.

(6) Chatterjee, N.; Walker, G. C. *Environ. Mol. Mutagen.* **2017**, *58*, 235-263.

(7) Kasai, Hiroshi; Nishimura, S. *Nucleic Acids Res*. **1984**, *12*, 2137-2145.

(8) Dizdaroglu, M. *Biochem J.* **1986**, *238*, 247-254.

(9) Kasai, H.; Nishimura, S. *Environ. Health Perspect*. **1986**, *67*, 111-116.

(10) Kasai, H; Crain, P. F.; Kuchino, Y.; Nishimura, S.; Ootsuyama, A.; Tanooka, H. *Carcinogenesis* **1986**, *11*, 1849-1851.

(11) Kasai, H.; Nishimura, S.; Kurokawa, Y.; Hayashi, Y. *Carcinogenesis* **1987**, *8*, 1959-1961.

(12) Ames, B. N.; Gold, L. S. *Mutation Research* **1991**, *250*, 3-16.

(13) Abu-Shakra, A.; Gold, B. *Nucleic Acids Res*. **2011**, *39*, 6789-6801.

(17) Nakabeppu, Y. *Int. J. Mol. Sci*. **2014**, *15*, 12543-12557.

(18) Shibutani, S.; Takeshita, M.; Grollman, A. P. *Nature* **1991**, *349*, 431-434.

(19) Anderson, M. W.; Reynolds, S. H.; You M.; Maronpot, R. M. *Environ. Health Pespect*. **1992**, *98*, 13-24.

(20) Kozmin, S. G.; Sedletska, Y.; Reynaud-Angelin, A.; Gasparutto, D.; Sage, E. *Nucleic Acids Res*. **2009**, *37*, 1767-1777.

(21) Lu, R.; Nash, H. M.; Verdine, G. L. *Curr. Biol*. **1997**, *7*, 397-407.

(22) Nakabeppu, Y. *Prog. Nucleic Acid Res. Mol. Biol.* **2001**, *68*, 75-94.

(23) Bauer, N. C.; Corbett, A. H.; Doetsch, P. W. *Nucleic Acids Res*. **2015**, *43*, 10083-10101.

(24) Zhang, Y.; Rohde, Larry, H.; Wu, H. *Current Genomics* **2009**, *10*, 250-258.

(25) Klungland, A.; Rosewell, I.; Hollenbach, S.; Larsen, E.; Daly, G.; Epe, B.; Seeberg, E.; Lindahl, T.; Barnes, D. E. *Proc. Natl. Acad. Sci. USA* **1999**, *96*, 13300-13305.

(26) Osterod, M.; Hollenbach, S.; Hengstler, J. G.; Barnes, D. E.; Lindahl, T.; Epe, B. *Carcinogenesis* **2001**, *22*, 1459-1463.

(27) Mahjabeen, I.; Ali, K.; Zhou X.; Kayani, M. A. *Tumor Biol*. **2014**, *35*, 5971-5983.

(28) Ali, K.; Mahjabeen, I.; Sabir, M.; Mehmood, H.; Kayani, M. A. *Dis. Markers*, **2015**, 690878.

(29) Sugimura, H.; Kohno, T.; Wakai, K.; Nagura, K.; Genka, K.; Igarashi, H.; Morris, B. J.; Baba, S.; Ohno, Y.; Gao, C.; Li, Z.; Wang, J.; Takezaki, T.; Tajima, K.; Varga, T.; Sawaguchi, T.; Lum, J. K.; Martinson, J. J.; Tsugane, S.; Iwamasa, T.; Shinmura, K.; Yokota, J. *Cancer Epidemiol. Biomarkers Prev.* **1999**, *8*, 669-674.

(30) Zhong, D.; Li, G.; Long, J.; Wu, J.; Hu, Y. *Sci. Rep.* **2012**, *2*, 548.

(31) Das, S.; Nath, S.; Bhowmik, A.; Ghosh, S. K.; Choudhury, Y. *Springerplus*. **2016**, *29*, 227

(32) Bacsi, A.; Aguilera-Aguirre, L.; Szczesny, B.; Radak, Z.; Hazra, T. K.; Sur, S.; Ba, X.; Boldogh, I. *DNA Pepair* ***2013***, *12*, 18-26.

(33) Aguilera-Aguirre, L.; Bacsi, A.; Radak, Z.; Hazra, T. K.; Mitra, S.; Sur, S.; Brasier, A. R.; Ba, X.; Boldogh, I. *J. Immunol.* **2014**, *193*, 4643-4653.

(34) Chen, S. Y.; Wan, L.; Huang, C. M.; Huang, Y. C.; Sheu, J. J. C.; Lin, Y. J.; Liu, S. P.; Lan, Y. C.; Lai, C. H.; Lin, C. W.; Tsai, C. H.; Tsai, F. J. *Rheumatol. Int.* **2012**, *32*, 1165-1169.

(35) Donley, N.; Jaruga, P.; Coskun, E.; Dizdaroglu, M.; McCullough, A.; K.; Lloyd, R. S. *ACS Chem. Biol.* **2015**, *10*, 2334-2343.

(36) Testa, B.; Mayer, J. M. *Hydrolysis in Drug and Prodrug Metabolism Chemistry, biochemistry and enzymology*, Wiley-VCH, Weinheim, **2003**, Chapter 4, 148-162.

(37) Sugiyama, H.; Kawabata, H.; Fujiwara, T.; Dannoue, Y.; Saito, I. *J. Am. Chem. Soc.* **1990**, *112*, 5252-5257.

(38) Chowdhury, G.; Guengerich, F. P. *Chem. Res. Toxicol*. **2009**, *22*, 1310-1319.

(39) Edwards, S. K.; Ono, T.; Wang, S.; Jiang, W.; Franzini, R. M.; Jung, J. W.; Chan, K. M.; Kool, E. T. *ChemBioChem* **2015**, *16*, 1637-1646.

(40) Beharry, A. A.; Lacoste, S.; O'Connor, T. R.; Kool, E. T. J. Am. Chem. Soc. 2016, 138, 3647-3650.

(41) Sloss, M. K.; Mckenna, J.; Yoon, W. H.; Norris, S.; Robinson, D.; Parnes, J. Shevlin, G. WO2009089042.

(42) Rashad, A. A.; Jones, A. J.; Avery, V. M.; Baell, J.; Keller, P. A. *ACS. Med. Chem. Lett.* **2014**, *5*, 496-500.

(43) Katagiri, K.; Sakai, T.; Hishikawa, M.; Masu, H.; Tominaga, M.; Yamaguchi, K.; Azumaya, I. *Cryst. Growth Des.* **2014**, *14*, 199-206.

(44) Lipinski, C. A.; Lombardo, F.; Dominy, B. W.; Feeney, P. J. *Adv. Drug Del. Rev.* **1997**, *23*, 3-25.

(45) Cox, P. B.; Gregg, R. J.; Vasudevan, A. *Bioorg. Med. Chem.* **2012**, *20*, 4564-4573.

(46) Mohan, C.; Long, K. D.; Mutneja, M. *An Introduction to Inhibitors and Their Biological Applications*, EMD MILLIPORE, Billerica, **2013**, 3-22.

(47) Yoshimoto, K.; Nishizawa, S.; Minagawa, M.; Teramae, N. *J. Am. Chem. Soc*. **2003**, *125*, 8982-8983.

(48) Rees, W. A.; Yager, T. D.; Korte, J.; von Hoppel, P. H. *Biochemistry* **1993**, *32*, 137-144.

(49) Carter, M.; Jemth, A.-S.; Hagenkort, A.; Page, B. D. G.; Gustafsson, R.; Griese, J. J.; Gad, H.; Valerie, N. C.K.; Desroses, M.; Boström, J.; Berglund, U. W.; Helleday, T.; Stenmark, P. *Nat. Commun*. **2015**, *6*, 7871.

(50) Cedergren-Zeppezauer, E. S.; Larsson, G.; Nyman, P. O.; Dauter, Z.; Wilson, K. S. *Nature* **1992**, *355*, 740-743.

(51) Iyama, T.; Abolhassani, N.; Tsuchimoto, D.; Nonaka, M.; Nakabeppu, Y. *Nucleic Acids Res*. **2010**, *38*, 4834-4843.

(52) Yang, C.-G.; Yi, C.; Duguid, E. M.; Sullivan, C. T.; Jian, X.; Rice, P. A.; He, C. *Nature* **2008**, *452*, 961-965.

(53) Sundheim, O.; Vågbø, C. B.; Bjørås, M.; Sousa, M. ML.; Talstad, V.; Aas, P. A.; Drabløs, F.; Krokan, H. E.; Tainer, J. A.; Slupphaug, G. *EMBO J*. **2006**, *25*, 3389-3397.

(54) Zhang, Z.; Shen, J.; Yang, Y.; Li, J.; Cao, W.; Xie, W. *ACS Chem. Biol*. **2016**, *11*, 1729-1736.

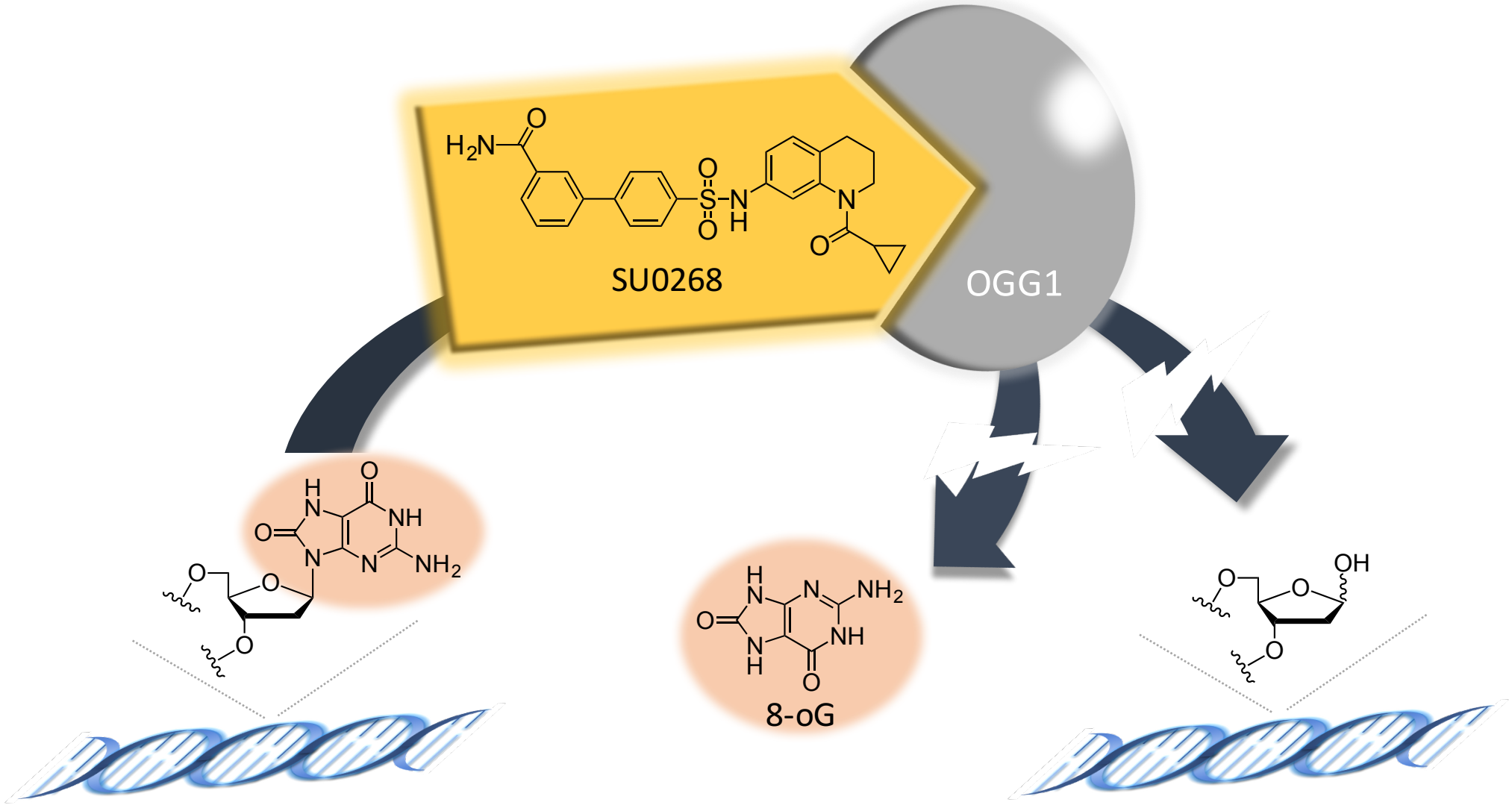
SU0268
OGG1
8-oG